13th International Conference on
Structural Health Monitoring of Intelligent Infrastructure

DOI: 10.3217/978-3-99161-057-1-106

Smart Pavement Subsurface Monitoring with Distributed Embedded Passive RF Sensor Network

Kent X. Eng[1], Zygmunt J. Haas[2], Samir R. Das[3], Petar Djurić[4], Milutin Stanaćević[3], Branko Glisic[1]
[1]Princeton University, Department of Civil and Environmental Engineering, Princeton, NJ, 08544, USA
[2]University of Texas at Dallas, Department of Computer Science and Cornell University, School of Electrical and Computer Engineering, Richardson, TX, 75080, USA
[3]Stony Brook University, Department of Electrical and Computer Engineering, Stony Brook, NY, 11794, USA
[4]Stony Brook University, Department of Computer Science, Stony Brook, NY, 11794, USA
email: ke9722@princeton.edu, zjh130030@utdallas.edu, samir@cs.stonybrook.edu, petar.djuric@stonybrook.edu, milutin.stanacevic@stonybrook.edu, bglisic@princeton.edu

ABSTRACT: Pavement subsurface deterioration can lead to catastrophic road failures, often caused by long-term settlements and moisture accumulation. These effects develop gradually and are difficult to identify through manual inspection. Although structural health monitoring (SHM) systems have been developed to address these challenges, most are insufficient to collect 3D spatial information due to their limitations. Current systems primarily focus on surface and base courses, neglecting subsurface courses which sustain loads and provide stability. Therefore, it is essential to develop a long-term and scalable monitoring system for subsurface courses. Radio frequency sensing system has great potential to fill the gap.

This study aims to further quantify the uncertainty of using distributed embedded passive radio frequency (RF) sensors in pavement subsurface courses. Laboratory experiments were conducted to investigate the uncertainty sources of the relationships between channel information and structural changes. Key challenges include correlating collected data with subsurface changes and finding the sources of uncertainties.

The results demonstrate the effect of system topology on the relationships between channel information and structural changes. These prove the system's applicability in subsurface spatial monitoring. By addressing implementation challenges and decoupling monitored parameters, the system could be further advanced for real-world deployment
KEY WORDS: Structural health monitoring; Transportation monitoring; Pavement monitoring; RF sensing; Sensor network

1 INTRODUCTION

Pavement road structures are essential and critical infrastructure to the urban transportation system. However, aging, massive urbanization, and overuse contribute to distress and even catastrophic failure events. For example, part of California State Route 1, which was 150 feet long, was washed out in a landslide, which led to the total cost of repairing and clearing being $11.5 million [1]. Meanwhile, the ASCE report card states that the grading evaluation on pavement roads is D+ [2]. Structural health monitoring systems can identify the pavement road's deterioration or damage at an early stage, which reduces economic loss and increases life safety.

Structural health monitoring (SHM) systems face a challenge in extracting large-scale spatial information in pavement subsurface courses at a reasonable cost. Current techniques are mainly limited to extracting one-dimensional or two-dimensional information from the structure [3]. However, extracting three-dimensional information gathered throughout the volumes of structural material, such as detection, location, and quantification of distress behaviors (e.g., damage, deterioration, or loss of performance) at an early stage is impossible using current SHM techniques. Meanwhile, most SHM systems primarily focus on the surface and base courses instead of the subsurface course, which sustains loads and provides stability. Therefore, it is essential to develop a 3D spatial monitoring system for long-term and scalable subsurface course monitoring. The recent developments in radio frequency (RF) sensing can be the potential solution to the challenges.

Recent research on radiofrequency (RF) sensing has resulted in hardware systems potentially suitable for the use in subsurface SHM [4]. RF sensors leverage channel information to monitor the 3D distribution of key parameters. A recent experiment demonstrates the feasibility of monitoring deformation and water content [5]. However, the uncertainty of monitoring deformation and water content has never been investigated. This study aims to investigate the uncertainty of monitoring deformation and water content using an RF sensing system.

2 UNCERTAINTY IN DECODING

Previous studies have shown that the displacement of sensors (measurand) is linearly related to the phase shift (encoding parameter) of the reflected signals. However, in the implementation scenarios, the exciter, which sends power to sensors, is mobile, and the sensors may have different initial mutual distances. The linear relationship, necessary to decode displacement from RF phase shift, can be affected by these different exciter locations and the initial distances between sensors. Therefore, the uncertainty in encoding function due to variable exciter locations and the initial distances between the sensors has to be investigated.

2.1 Method

A set of experiments was performed to determine the change of displacement between sensors in various 1D settings, where the backscatter RF signal propagated through the air. The goal of the experiment setup was to verify the effects of exciter locations and the initial distance of sensors. The 1D experiments consisted of two sensors and one exciter. The

DOI: 10.3217/978-3-99161-057-1-106

exciter was used to power the two sensors wirelessly. One sensor was placed on the mobile tripod which was installed on a camera slider such that the mobile tripod was displaced by a linear actuator along the slider. Another sensor was placed on a stationary platform. The two sensors were set up with three different initial distances D: 30 cm, 60 cm, and 126 cm. At each setup of D, the mobile sensor was displaced by the linear actuator with a change in distance Δd = 1 cm at a time while the static sensor remained stationary. After each 1 cm displacement, data were collected for 10 minutes with a sample rate of 30 seconds. The total displacement was 16 cm. After the experiments were conducted with three different D, the exciter was moved to a different location with repeated experiments of the different initial distances. By varying the initial distance, the effect of different initial distances between sensors on the linear (decoding) relationship could be investigated. By changing the exciter location, the effect of variable exciter location on the linear relationship could be investigated. These experiments can also show which effects have a larger impact on the linear relationship between displacement and phase shift. The experimental setup was shown in Figure 1. The antenna icon represents the location of the sensors, and the left sensor was the mobile sensor. The star represents the locations of exciters for each experiment. A total of 12 experiments were conducted (three initial distance setups with four different exciter locations).

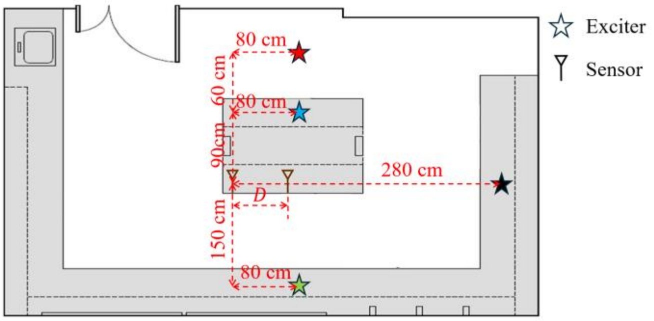

Figure 1. Location of the sensor and various exciters for the experimental setup in the indoor laboratory

2.2 *Discussion*

For each experiment, a linear relationship was obtained by fitting the median value of the recorded phase shift at each displacement, as shown in Figure 2. The slope of the linear fitting line represented the sensitivity of the system (the ratio between phase shift and displacement) $\widehat{\Delta\theta/\Delta d}$.

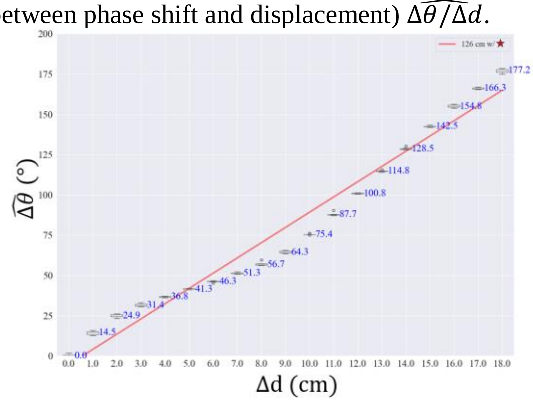

Figure 2. Experimental result of D = 126 cm and the exciter location (red star); the red line indicated the linear fitting line

Table 1. $\widehat{\Delta\theta/\Delta d}$ (°/cm) Comparison

D	Red Star	Blue Star	Green Star	Black Star	Max Min Diff. (%)
30 cm	10.17	10.45	10.11	10.34	3.4
60 cm	9.96	10.02	10.19	10.06	2.3
126 cm	9.54	9.86	11.48	10.87	**20.3**
Max Min Diff. (%)	6.6	5.98	**13.6**	8.05	

The results of 12 experiments are shown in Table 1. Maximum and minimum differences were also calculated across different exciter locations and sensor distances D. The maximum and minimum difference of each D showed that as D increased, the difference in $\widehat{\Delta\theta/\Delta d}$ also increased. This demonstrated that the variation of $\widehat{\Delta\theta/\Delta d}$ increased as the initial distance between sensors increased. The maximum and minimum difference of each location showed that the largest variation occurred when the excited was located at the green star, perpendicular to the communication line between sensors. However, this phenomenon was observed only with the case of D = 126 cm. If the case of D = 126 cm was removed, the variation of $\widehat{\Delta\theta/\Delta d}$ was similar across different exciter locations. The initial distance between sensors was more impactful to the variation of $\widehat{\Delta\theta/\Delta d}$ comparing to the exciter location.

The linear fitting errors were also investigated in these experiments. As shown in Figure 2, the fitting error was presented in the linear fitting line. The variation of fitting errors across different D and exciter locations were shown in Table 2. The results showed that as the initial distance between sensors increased, the fitting error also increased. Meanwhile, the location of exciter had smaller effects on the fitting errors compared to the initial distances between sensors.

Table 2 Fitting error ($\widehat{\Delta\theta/\Delta d}$ error) comparison

D	Red Star	Blue Star	Green Star	Black Star
30 cm	**5.34**	**4.16**	**5.93**	**4.22**
60 cm	8.99	6.29	14.74	6.19
126 cm	15.42	17.84	18.54	16.98

The fitting error and the discrepancy of $\widehat{\Delta\theta/\Delta d}$ with various sensor spacing issues were potentially caused by the signal multipath effects. Since the experiments were conducted in an indoor laboratory, the surroundings reflected the backscattered signal from the transmitter sensor to the receiver sensor. The superposition of the backscattered signal and reflected signal can potentially affect the accuracy of the data collection. Additional experiments must be conducted to verify the causes.

In real applications, material inhomogeneity (e.g. moisture and density of fine aggregate) inside the structure can potentially affect the system's accuracy. Previous studies have demonstrated the capability of detecting the change of water content using an RF system [5]. Therefore, the material inhomogeneity due to moisture content can be further decoupled. Meanwhile, the effects from other sources of material inhomogeneity have to be further studied. Uncertainty quantification can be used to preliminarily quantify the effects of those sources.

DOI: 10.3217/978-3-99161-057-1-106

3 CONCLUSION

This study investigates the uncertainties in the relationship between the channel phase (encoding parameter) and displacement (measurand) registered by RF sensors. Although distributed embedded passive radio RF sensors have great potential for 3D spatial pavement subsurface monitoring, the relationship between measurand and encoding parameter can be affected by the initial distances between sensors. As the initial distance between sensors increases, the uncertainty in the relationship also increases. Meanwhile, the location of the exciter has a smaller effect on the relationship. The reason behind this finding will be the subject of future work.

ACKNOWLEDGEMENT

This research was funded by the National Science Foundation under Grants No. ECCS-2329800, ECCS-2329801, and ECCS-2329802. Any opinions, findings, and conclusions or recommendations expressed in this material are those of the authors and do not necessarily reflect the views of the National Science Foundation. The authors would like to thank Joseph Vocaturo Jr., Mauricio Pereira, Angel Dong, and Dane Utley for their help and contributions.

REFERENCES

[1] Caltrans, “Highway 1 at Rat Creek Reopened to Traffic at Noon on April 23,” California Department of Transportation. Accessed: Sep. 01, 2021. [Online]. Available: https://dot.ca.gov/news-releases/news-release-2021-013

[2] “2025 Infrastructure Report Card | ASCE’s 2025 Infrastructure Report Card,” ASCE’s 2025 Infrastructure Report Card |. Accessed: Mar. 30, 2025. [Online]. Available: https://infrastructurereportcard.org/

[3] S. Cola, V. Girardi, S. Bersan, P. Simonini, L. Schenato, and F. De Polo, “An optical fiber-based monitoring system to study the seepage flow below the landside toe of a river levee,” *J. Civ. Struct. Health Monit.*, vol. 11, no. 3, pp. 691–705, Jul. 2021, doi: 10.1007/s13349-021-00475-y.

[4] A. Ahmad, X. Sha, M. Stanaćević, A. Athalye, P. M. Djurić, and S. R. Das, “Enabling Passive Backscatter Tag Localization Without Active Receivers,” in *Proceedings of the 19th ACM Conference on Embedded Networked Sensor Systems*, in SenSys ’21. New York, NY, USA: Association for Computing Machinery, Nov. 2021, pp. 178–191. doi: 10.1145/3485730.3485950.

[5] K. X. Eng *et al.*, “A Vision and Proof of Concept for New Approach to Monitoring for Safer Future Smart Transportation Systems,” *Sensors*, vol. 24, no. 18, Art. no. 18, Jan. 2024, doi: 10.3390/s24186018.